Number 30
December 2006

SWISS NEUTRON NEWS

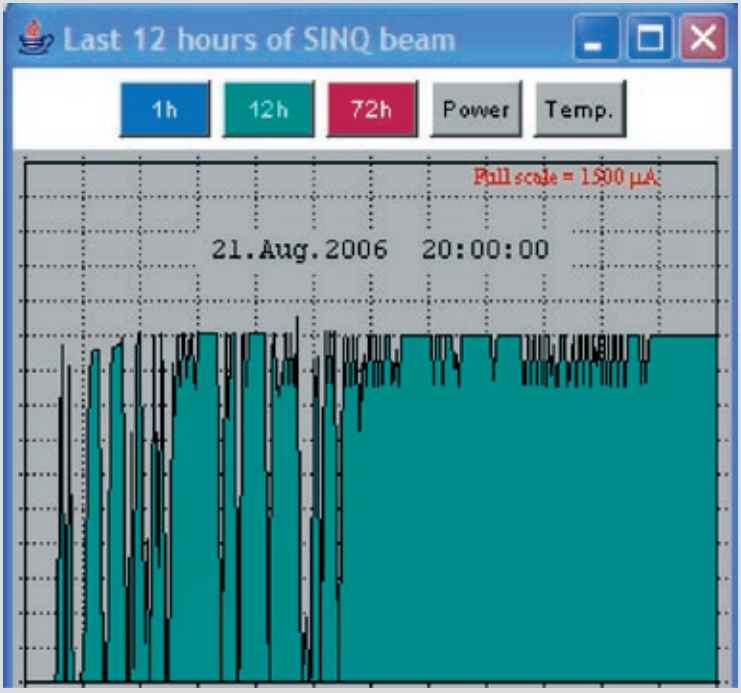

Schweizerische Gesellschaft für Neutronenstreuung
Société Suisse pour la Diffusion des Neutrons
Swiss Neutron Scattering Society

EDITORIAL:

Editor: Swiss Neutron Scattering Society

Board for the Period January 2004 – January 2007:

President:	Dr. P. Allenspach	peter.allenspach@psi.ch
Board Members:	Prof. Dr. S. Decurtins	silvio.decurtins@iac.unibe.ch
	Prof. Dr. B. Schönfeld	schoenfeld@iap.phys.ethz.ch
Secretary:	Dr. S. Janssen	stefan.janssen@psi.ch
Honorary Members:	Prof. Dr. W. Hälg, ETH Zürich	
	Prof. Dr. K.A. Müller, IBM Rüschlikon and Univ. Zürich	
	Prof. Dr. A. Furrer, ETH Zürich and Paul Scherrer Institut	
Auditors:	Dr. W. Fischer, Paul Scherrer Institut	
	Dr. K. Krämer, University of Berne	
Address:	Sekretariat SGN/SSDN	
	Paul Scherrer Institut	
	bldg. WLGA/002	
	5232 Villigen PSI, Switzerland	
	phone:	+41-(0)56 - 310 4666
	fax:	+41-(0)56 - 310 3294
	www:	http://sgn.web.psi.ch
Bank Account:	Postfinance:	50-70723-6
	BIC:	POFICHBE
	IBAN:	CH39 0900 0000 5007 0723 6
Printing:	Paul Scherrer Institut	
Circulation:	2100, 2 numbers per year	
Copyright:	SGN/SSDN and the respective authors	

ON THE COVER:

History of the first 12 hours of Megapie neutron beam when normal user operation had started on August 21st.

// Contents //

// The President's Page //

DEAR MEMBERS

The liquid SINQ-target MEGAPIE successfully finished its operation just before Christmas and we can say that it performed well beyond expectation with up to 80% more neutrons and only very minor technical problems. All the previous pundits I know (and I was one of them) have adjusted their views by this very positive experience to full supporters of future liquid targets for SINQ. I would like to congratulate PSI and all people involved for this marvelous experiment. The next target will again be a solid target, but for the first time, one with all rods made out of Zirkalloy. This should result in an increased flux compared to the steel rods of the order of 20%. With this target type built in, with the development of a new liquid target going ahead and with a planned power upgrade of the proton accelerator, SINQ can be expected to remain a competitive neutron source for the years to come. With MARS being commissioned at the moment, FOCUS-SANS to be installed this winter, EIGER entering construction phase, DMC-II being approved and the gradual upgrades on all the other instruments, it is also assured that the neutrons produced in SINQ are used in the most efficient way.

In the last Swiss Neutron News issue I informed you about this planned workshop about the instrumentation on a long pulse target station (LP-TS) ESS, which then took place in Rencurel. I have to confess that based on the updated Volume 3 of the ESS report I regarded the LP-TS as a compromise especially in the field of spectroscopy. However, as a result of the workshop and the many simulations, which have been performed there, I had to revise my opinion. The combination of low repetition rate, the implementation of pulse shaping choppers and the long distances to the instruments allow for a flexible choice of resolution and increase of intensity by multiplexing. Besides high resolution backscattering and eV-spectroscopy such a 5MW

LP-TS will easily beat a 1MW short pulse TS and in addition comprises less technical uncertainties.

Another positive development was the publication of the ESFRI-roadmap which includes the ILL-upgrade and the ESS-project (5MW LP-TS). This publication caused a lot of actions, which now have been channeled in a way to obtain a common momentum towards a realization of ESS. There is a lot of politics and vested interests involved, which might de-rail this process. I promise you that I will do whatever possible, as the president of SGN and in my new function as ENSA chairman, to help the process to go ahead in the right direction.

// Peter Allenspach

// Hans U. Güdel retired in autumn 2006 //

A. Furrer
Laboratory for Neutron Scattering, Paul Scherrer Institut & ETH Zurich, CH-5232 Villigen PSI

Hans U. Güdel mainly before the year 2006.

The invitation to participate in the colloquium for Hans U. Güdel on July 7, 2006, at the Department for Chemistry and Biochemistry of the University of Berne came as a surprise, since nobody actually expected Hans to leave his faculty position before the normal age of retirement. However, Hans has always been unconventional during all his life, and his early retirement underlines again his attitude to do the unexpected rather than to follow the common rules. The speakers of the colloquium gave an almost complete overview on Hans' activities during the last four decades. The presence of numerous former students, collaborators, colleagues and friends demonstrated the great impact which Hans achieved during his active life as a dedicated researcher, as a gifted teacher, and as a highly appreciated advisor in many scientific committees and councils.

In November 2006, the ISI web of knowledge listed 521 refereed scientific articles which Hans published so far as author and co-author, and many more articles appeared in books and proceedings. This is an impressing scientific work covering a broad range of topics, and I am somehow proud that I had the opportunity to collaborate with Hans in some hundred out of these 521 articles. In the following I will go through some of the highlights of our scientific collaboration which was a truly interdisciplinary venture, because Hans received his university degrees in inorganic chemistry, whereas my scientific background is solid state physics. I feel that we nicely achieved to combine and to join the culture of the two disciplines in common

projects with great success, which was honoured through awarding the Walter Hälg Prize 2005 of the European Neutron Scattering Association (ENSA).

One coherent theme has been running through all our joint actvities, namely the study of low-dimensional magnetic systems and in particular magnetic cluster systems. The start in the mid-seventies was highly exciting; we were the first to measure directly the energy splittings of magnetic dimers and higher multimers (so-called magnetic clusters) by inelastic neutron scattering, see Phys. Rev. Lett. **39**, 657 (1977). Subsequently this work has served as a key reference in similar measurements performed by other groups, since it did not only demonstrate the feasibility of such experiments, but provided the theoretical basis for the data interpretation, as increasingly used today in the field of spin clusters including supramolecular nanomagnets, a field to which Hans has made essental contributions in recent years.

Neutron experiments on magnetic clusters provide direct information on the exchange interaction between the magnetic ions. In the past, the Heisenberg model has been widely used to describe exchange interactions in magnetic systems, although it inherently represents just a first approximation of the true situation. The presence of intrinsic higher-order terms was pointed out by Anderson in his famous article in *Magnetism* (Vol. 1) already in 1963. We started to search for such higher-order terms and found indeed direct spectroscopic evidence for an appreciable contribution of biquadratic exchange in neutron experiments on Mn pairs in the diluted one-dimensional magnet $Cs(Mn,Mg)Br_3$, see Phys. Rev. Lett. **52**, 1336 (1984). The nature of biquadratic exchange does not only involve pair interactions, but also three-body, four-body, etc. interactions if extended to higher clusters. Further neutron experiments on Mn trimer chain segments in $Cs(Mn,Mg)Br_3$ proved the existence of a true three-spin exchange term similar in magnitude to the corresponding biquadratic two-spin term, see Phys. Rev. Lett. **56**, 1956 (1986). This was a result of fundamental importance, since n-body interactions (n>2) have so far only been verified in solid ^3He, nuclear matter, and disordered binary alloys.

A particularly interesting system studied during the eighties was the spin-dimer compound $Cs_3Cr_2Br_9$, because it exhibits field-induced magnetic ordering when the singlet-triplet energy gap closes, thus Bose-Einstein condensation of the triplet states with a gapless Goldstone mode could be expected to occur. However, detailed field-dependent neutron scattering experiments showed that the lowest singlet-triplet excitation branch does not soften completely due to some inherent anisotropy, see Phys. Rev. B **30**, 6300 (1984); **31**, 597 (1985). Nevertheless, these experiments served as an excellent basis for the later observation of the Bose-Einstein condensation in $TlCuCl_3$.

In the late eighties Hans was searching for suitable materials to be used in the design of efficient up-conversion lasers. Compounds of composition $Cs_3R_2Br_9$ (R=rare earth) were found to be particularly well suited for this purpose. The electronic properties of these compounds are governed by the dimers of R ions built into the molecular unit, thus Hans approached me to study the corresponding

excitations. The neutron experiments performed for almost the whole R series provided completely unexpected results. The usual phenomenological models (Heisenberg, Ising, xy) failed to reproduce the observed energy spectra. However, an exchange-tensor formalism which takes into account the initial and final electronic states of the interacting ions, turned out to provide an excellent description, see Phys. Rev. Lett. **64**, 68 (1990). These experiments – together with the work on Mn dimers and trimers described above – convincingly demonstrated the shortcomings of the usual phenomenological approximations to describe the exchange interaction, whose true nature can only be unravelled if appropriately tailored experiments are performed.

In the nineties I was involved in investigations of the inhomogeneous materials properties of high-temperature superconductors. Motivated by the fact that suitably doped spin-ladder compounds such as $Ca@Sr_{14}Cu_{24}O_{41}$ become superconducting under pressure, I initiated a co-operation with Hans to study the novel S=1/2 spin-ladder compounds $ACuCl_3$ (A=K, Tl, NH_4) for which his group had the necessary expertise in the synthesis and growth of single crystals. In a first step the dispersion of the magnetic excitations was established for $KCuCl_3$ by inelastic neutron scattering, see Eur. Phys. J. *Rapid Note* B **7**, 519 (1999). Surprisingly, the magnetic excitations turned out to be dispersive in all directions of reciprocal space (i.e., not only along the ladder direction as anticipated)

Hans U. Güdel mainly after the year 2006.

with structure factors imaging the nearest-neighbour Cu pair distance, thereby proving that this compound series has the properties of an S=1/2 spin-dimer rather than a spin-ladder compound. The experiments were then extended to investigate the magnetic field dependence of the singlet-triplet excitation including the isostructural compound $TlCuCl_3$, see Phys. Rev. B **65**, 132415 (2002). Based on these experiments we realised that the field-driven quantum criticality can indeed be reached in these systems, and for the first time the picture of the Bose-Einstein condensation of magnons in $TlCuCl_3$ could be verified, see Nature **423**, 62 (2003).

Neutron scattering was a key technique in many scientific works in which Hans has been involved. However, Hans was not only a mere user and consumer of neutrons, but he also made tremendous efforts to provide excellent experimental opportunities for the Swiss neutron scattering community as a whole. In the mid-eighties, he was one of the initiators of the Swiss partnership with the Institute Laue-Langevin (ILL) in Grenoble which runs the world's most powerful neutron source (Hans is presently the Swiss member in the Scientific Council of the ILL). He then realized that the voice of the users has to be articulated in a focused manner, thus he was pushing this idea, and he was the founding Chairman when the Swiss Society for Neutron Scattering was created on 25 October 1991 in Berne. Hans strongly supported also the idea of a Swiss home base in neutron scattering, namely the spallation neutron source SINQ at PSI from the very beginning, first as convenor of the time-of-flight instrument group during the project phase and then as a member of the Scientific Committee after the start of the regular SINQ operation in 1998.

I very much enjoyed the co-operation with Hans in the last thirty years, and I will thankfully remember the numerous experimental campaigns and enlightning discussions with Hans and with many of his students who were always involved as a prerequisite in almost any of our common research projects. Hans, you can look back to an extremely successful career, and you can be sure that your purposive but yet unconventional way of doing research will be continued by your former students and collaborators as honestly demonstrated through all your scientific life. Fortunately, you still have your office in Berne, thus we may expect from you further surprises in research, yet at a slightly moderate pace due to some of your alternative activities such as tennis, curling, and mountain climbing which will probably gain in importance in the future. Hans, I cordially thank you for our past co-operation, and I wish you all the best for the bright future ahead of you.

// Metal-like elasticity in colloidal crystals //

U. Gasser[1*], D. Reinke[2], H. Stark[3], H.-H. von Grünberg[4], A. B. Schofield[5], G. Maret[2]

[1] Laboratory for Neutron Scattering, ETH Zurich & Paul Scherrer Institut, 5232 Villigen PSI, Switzerland

[2] Physics Department, University of Konstanz, 78457 Konstanz, Germany,

[3] Max-Planck-Institut für Dynamik und Selbstorganisation, Bunsenstr. 10, D-37073 Göttingen, Germany,

[4] Karl-Franzens-Universität, 8010 Graz, Austria,

[5] School of Physics, University of Edinburgh, Edinburgh, Scotland EH9 3JZ, UK,

** To whom correspondence should be addressed; E-mail: urs.gasser@psi.ch*

In a recent study *(1)*, the elastic properties of single crystals consisting of charged colloidal particles were determined from real-space imaging experiments using confocal microscopy. The normal modes and the force constants of the crystal were obtained from the fluctuations of the particle positions around the lattice sites using the equipartition theorem. We show that the elasticity of the studied crystals is largely analogous to that of metals. Like the conduction electrons in metals, the small ions in the solvent of the colloidal crystals give rise to non-central forces between the big colloidal particles and, therefore, the Cauchy relation is not fulfilled.

Understanding how an elastic material deforms under external mechanical stresses is essential knowledge in material science and of fundamental interest. The elastic properties of a crystal as well as the interactions between the particles forming a crystal lattice are character-ized by force constants *(2,3)*. These relate the displacement of one particle from its equilibrium position to the force acting on a neighboring particle. In metallic and other hard crystalline materials a great deal is known about these microscopic forces and about elasticity. However, in soft materials such as colloidal suspensions the study of elasticity currently receives a lot of attention because of their great potential for the development of novel materials with tailored properties. Yet, the elastic constants of colloidal crystals have never been measured and the nature of the internal forces in colloidal crystals is largely unknown.

In analogy to metals, crystals of charged colloids *(4)* consist of mesoscopic, Brownian macroions in suspension that form a lattice and are surrounded by the much smaller microions. Like the electrons in metals, the

microions are much more mobile than the large ions that form the lattice and, as a consequence, they always arrange in clouds around the macroions to screen their charges. Thus, in metals and crystals of charged colloids there are two species that move and respond on vastly different length and time scales. Therefore, the question arises whether these similarities manifest themselves in similar elastic properties despite the huge difference in the respective moduli.

Information on the nature of the interactions in colloids can be obtained by measuring the components of the tensor of elasticity. These are defined as the second derivatives of the elastic free energy of a crystal with respect to components of the strain tensor: $C_{\mu\nu\rho\sigma} = \partial^2 F / \partial\eta_{\mu\nu}\partial\eta_{\rho\sigma}$ *(3)*. The number of independent components of $C_{\mu\nu\rho\sigma}$ depends on the point symmetry of the crystal; a crystal with the cubic *fcc* symmetry has only three independent elastic constants: C_{11}, C_{12}, and C_{44}, where the indices are given in Voigt notation *(3)*. In 1828 A.J. Cauchy found that the assumption of central forces between small volume elements of a crystal yields additional relations between the elastic constants and, therefore, further reduces the number of independent components in $C_{\mu\nu\rho\sigma}$ *(2,5)*; e.g. for a crystal with *fcc* symmetry $C_{12} = C_{44}$ for central forces. These relations are now known as Cauchy relations, and they allow the interesting conclusion that their violation must be due to non-central forces. Metals are a good example: Because of non-central forces due to the conduction electrons that screen the charges of the ions the Cauchy relations are not fulfilled *(2)*.

In a recent study *(1)* we have shown that the elastic constants of colloidal crystals and essential information about the interactions between the colloidal particles can be obtained best by real-space imaging experiments. The experimental means for this have recently become available with fast laser scanning confocal microscopes. As illustrated in Fig. 1, our 3D realspace imaging data allows the direct observation and quantitative analysis of the structure and dynamics of up to

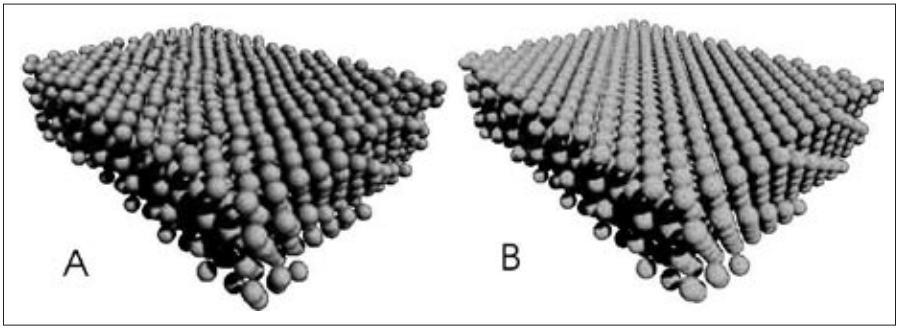

Fig. 1: (A) A snapshot of 1909 particles in a colloidal crystal with fcc symmetry. The image is obtained using the coordinates extracted from 100 2D microscopy images.
(B) A time average of the same crystal as shown in (A) calculated from 98 snapshots. The high quality of the crystal is apparent. In comparison with (A) the fluctuations of the particles around their equilibrium positions can be visualized.

10^4 micron-sized particles. From measurements of colloidal mono-crystals with *fcc* symmetry we extract the force constants of the crystal from the dispersion curves of overdamped normal modes and, in the $q \rightarrow 0$ limit, all elastic constants of the crystal. Our results show that the interaction between the colloidal particles in the crystal cannot be described in terms of central forces, but non-central forces acting between the macroions make the elastic response of the studied colloidal crystals similar to that of metals. In metals, the force constants can be determined with scattering methods such as inelastic neutron scattering that probe the normal modes of the lattice. However, in colloidal crystals scattering methods such as dynamic light scattering (DLS) do not yield the same information *(6,7)*, because the solvent of the suspension strongly damps the motion of the colloidal particles and, therefore, prevents the existence of propagating lattice normal modes. As a consequence, in scattering experiments, the force constants are always intertwined with the complicated, wave-vector dependent frictional forces with the solvent. In contrast to DLS, hydrodynamics does not play any role in the determination of the lattice normal modes from the real-space imaging data. Our method *(8)* relies exclusively on "snapshots" of the particle positions that are used to calculate ensemble averages and, therefore, the frictional forces between the colloidal particles and the solvent never enter our analysis.

We used poly-methylmethacrylate spheres *(9)* with a diameter σ = 1.66 μm that were fluorescently labeled with rhodamine and suspended in a solvent matching both density and refractive index of the particles. The particles were observed with a fast laser-scanning confocal microscope using a 100 × objective lens to observe a volume V ≈ 58 μm × 55 μm × 20 μm inside the much larger sample cell. The objective was mounted on a piezo translation stage for the scanning in z-direction and, typically, 5000 particles were observed in one 3D snapshot. It took ≈ 1.5 s to observe the whole volume V. After the experiment, the particles are detected by looking for local intensity maxima and their positions can be determined with an accuracy of ≈ 20nm *(10)*. Samples with volume fractions $0.01 < \phi < 0.41$ were prepared in order to map out the phase behavior at room temperature; all measurements were carried out at T = 295K. Crystallization was observed in samples with volume fractions larger than $\phi_f \approx 0.31$. The phase behavior compares well with that of hard spheres with Yukawa repulsion (HSY) with the interaction potential $V(r) = V_{HS}(r) + \frac{B\sigma}{r}\exp(-\kappa[r-\sigma])$ *(11)*. Here, $V_{HS}(r)$ is the hard sphere potential, $\kappa^{-1} = 221 \pm 30$nm is the Debye screening length, and $B = k_BT\frac{\lambda_B}{\sigma}\left(\frac{Z_{eff}}{1+\kappa\sigma/2}\right)^2 \approx 12k_BT$ is the contact value with the Bjerrum length λ_B and the charge number $Z_{eff} = 245 \pm 40$.

For $\phi \geq 0.31$ large random hexagonal close packed crystals *(12)* with hexagonal planes oriented parallel to the cover slip formed within several days, and we chose regions of three to ten hexagonal layers with *fcc*-stacking for our measurements. The lattice constant *a* of the Bravais unit cell was measured, and the structure of these crystals was compared with a perfect *fcc* lattice. As illustrated by Fig. 1B, the deviations of the average particle positions from the *fcc*-lattice positions

are small. For the calculation of the displacement $\mathbf{u}_i(t) = \mathbf{r}_i(t) - \mathbf{R}_i$ of particle *i*, the reference position $\mathbf{R}_i$ is determined by averaging its position over all snapshots taken during the measurement. The distributions of the components u_μ of the displacements are found to be Gaussian at all volume fractions, so we are always in the harmonic regime of crystal elasticity. Following essentially the same procedure as in Ref. *(8)*, the dynamical matrix $D_{\mu\nu}(\mathbf{q})$ *(2)* is determined using the equipartition theorem; each **q**-mode of the harmonic approximation $U = \frac{1}{2}\sum_{\mathbf{q},\mu,\nu} u_\mu(\mathbf{q})\, D_{\mu\nu}(\mathbf{q})\, u^*_\nu(\mathbf{q})$ to the elastic energy of the crystal contains the thermal energy $k_BT/2$. Therefore, the inverse of the dynamical matrix can be obtained from an ensemble average of the measured particle displacements:

$$D^{-1}_{\mu\nu}(\mathbf{q}) = \frac{\langle u_\mu(\mathbf{q}) u^*_\nu(\mathbf{q})\rangle}{k_BT} \qquad (1)$$

We calculate the ensemble average $\langle \ldots \rangle$ by taking a time average over all measured configurations and we analyze modes with wave vectors $\mathbf{q} \propto (1, 1, 0)$, $(1, 1, 1)$, and $(1, 0, 0)$. Since these directions in reciprocal space correspond to symmetry axes of 2-, 3-, and 4-fold rotations, the eigenmodes in these directions are a longitudinal mode *l* and two transverse modes t_1 and t_2 with eigenvectors $\hat{e}_l$, $\hat{e}_{t1}$, and $\hat{e}_{t2}$, respectively. As shown in Fig. 2, we obtain the modes *l*, t_1, and *s* with propagation $\mathbf{q} \propto (1, 1, 0)$, t_1 and m for $\mathbf{q} \propto (1, 0, 0)$, and t_1 and *m* for $\mathbf{q} \propto (1, 1, 1)$. Here, *s* denotes a combination of the modes t_1 and t_2, and *m* refers to a combination of longitudinal and transverse modes. The full lines represent fits with general force constants of an *fcc* lattice with interactions up to 3rd nearest neighbors. Three force constants ($A^{(1)}_{11}$, $A^{(1)}_{12}$, $A^{(1)}_{33}$) determine the forces between nearest neighbors, while two ($A^{(2)}_{11}$, $A^{(2)}_{22}$) and four ($A^{(3)}_{11}$, $A^{(3)}_{12}$, $A^{(3)}_{13}$, $A^{(3)}_{22}$) constants define the forces acting on the 2nd and 3rd neighbors, respectively (2). The absolute values of the 3rd order constants $A^{(3)}_{\mu\nu}$ are found to be ~ 0.01 $|A^{(1)}_{11}|$; they are not essential for the quality of the fits. For a radially symmetric interaction, the force constants fulfill the condition $\Gamma := A^{(1)}_{12} / (A^{(1)}_{11} - A^{(1)}_{33}) = 1$ *(2)*. However, from the measurements we find $\Gamma < 0.25$ at all ϕ. This is clearly incompatible with a pairwise additive, radially symmetric interaction. Furthermore the determined force constants differ strongly from those expected for a HSY-crystal. E.g.

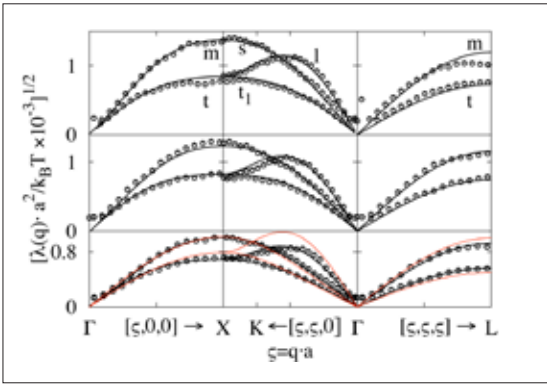

Fig. 2: Measured dispersion relations for (top to bottom) ϕ = 0.38, 0.34, and 0.31. The full lines represent fits to the data. K, X and L denote the edge of the 1st Brillouin zone in (1, 1, 0), (1, 0, 0), and (1, 1, 1)-direction, respectively. For each column, the modes are identified in the topmost panel. For comparison, the dispersion relations for a HSY crystal with $B = 15\, k_BT$ and $\kappa\sigma = 8$ are shown by the dotted lines for ϕ = 0.31. See text for details.

a displacement of the particle at (0, 0, 0) in the (1, 0, 0)-direction strongly attracts the 2nd neighbor at (*a*, 0, 0); this behavior is a consequence of many body forces and cannot be accounted for by the HSY interaction or any other radially symmetric pair potential. Potential error sources such as random errors in the particle coordinates, the effect of the finite scanning speed, the limited number of snapshots in a measurement, and the size of the observed volume *V* were assessed by comparing the measurements with MC simulations. The measurements were found to give reliable results *(1)*.

Therefore, we can determine all elastic constants of a colloidal crystal from a single measurement. In the $q \to 0$ limit, we obtain the tensor $B_{\mu\nu\rho\sigma}$, which connects stress and strain: $T_{\mu\nu} = B_{\mu\nu\rho\sigma}\,\varepsilon_{\rho\sigma}$. For crystals under stress, $B_{\mu\nu\rho\sigma}$ is not the same as the tensor of elastic constants $C_{\mu\nu\rho\sigma}$, which is defined via the elastic free energy *(3)*. The studied crystals are under stress due to the pressure *p* in the sample cell; for *fcc* symmetry the two tensors are connected by the relations $B_{11} = C_{11} - p$, $B_{12} = C_{12} + p$, and $B_{44} = C_{44} - p$ with the indices given in Voigt notation *(3)*. For central forces and cubic lattices, the condition $\Gamma = 1$ is a consequence of the Cauchy relation $B_{12} = B_{44} + 2p$. Elastic constants $B_{\mu\nu}$ and elastic moduli representative of all our results are shown in Table 1 along with values for a HSY crystal. Since $B_{44} > B_{12}$ and $p > 0$, our measurements clearly contradict the Cauchy relation, while it holds in HSY crystals. In analogy to metals, the non-centrality of the forces affects mostly the bulk modulus $K = (B_{11} + 2B_{12})/3$, while the shear moduli $G_1 = B_{11} - B_{12}$ and $G_2 = B_{44}$ have similar values in the studied crystals and HSY crystals. The value of *K* obtained from experiment is almost a factor of 3 smaller than for the HSY crystal. These observations corroborate that the micro-ions in crystals of charged colloids play a role similar to the electron gas in metals.

Our main results are the incompatibility of the force constants with any effective, radially symmetric pair-potential and the importance of many-body forces. The elastic properties and the behavior of the lattice normal modes in the studied colloidal crystals are rather metal- than HSY-like. Moreover, we note that direct observation of colloidal crystals yields the results that are obtained by e. g. inelastic neutron scattering in hard materials. Our methods are not limited to charged colloids but allow to study the elastic properties of various colloidal crystals that can be treated in the harmonic approximation.

This work has been supported by the Deutsche Forschungsgemeinschaft (DFG) through subproject C4 of the SFB TR6 program.

$\left(\frac{k_BT}{\sigma^3}\right)$	B_{11}	B_{12}	$B_{44} = G_2$	G_1	K
$\phi = 0.38$	67	17	65	50	33
$\phi = 0.34$	56	13	36	43	27
$\phi = 0.31$	28	9	28	19	15
HSY, $\phi = 0.31$	63	48	25	15	53

Table 1: Elastic constants $B_{\mu\nu}$ with indices given in Voigt notation and elastic moduli obtained from experiment and from a calculation for a HSY crystal ($B = 15\ k_BT$, $\kappa\sigma = 8$).

REFERENCES

1. D. Reinke *et al., Phys. Rev. Lett.* **98***, 038301 (2007)*.
2. P. Brüesch, *Phonons: Theory and Experiments I,* vol. 34 of *Springer Series in Solid-State Sciences* (Springer-Verlag, New York 1982).
3. D. C. Wallace in *Solid State Physics,* H. Ehrenreich, F. Seitz, D. Turnbull, Eds. (Academic Press, New York, 1970), vol. 25, pp. 301-404.
4. P. Pieranski, *Contemp. Phys.* **24**, 25 (1983).
5. A. J. Cauchy, *Exerc. de Math.* **4**, 129 (1828).
6. A. J. Hurd, N. A. Clark, R. C. Mockler, W. J. O'Sullivan, *Phys. Rev.* A **26**, 2869 (1982).
7. Z. D. Cheng, J. X. Zhu, W. B. Russel, P. M. Chaikin, *Phys. Rev. Lett.* **85**, 1460 (2000).
8. P. Keim, G. Maret, U. Herz, H.-H. von Grünberg, *Phys. Rev. Lett.* **92**, 215504 (2004).
9. L. Antl *et al., Colloids Surf.* **17**, 67 (1986).
10. J. C. Crocker, D. G. Grier, *J. Colloid Interface Sci.* **179**, 298 (1996).
11. A.-P. Hynninen, M. Dijkstra, *Phys. Rev. E* **68**, 021407 (2003).
12. P. N. Pusey et al., *Phys. Rev. Lett.* **63**, 2753-2756 (1989).

// Upgrade of the cold neutron diffractometer DMC at SINQ: Modern algorithms for calibration and integration of 2-D data //

A. Cervellino and L. Keller
Laboratory for Neutron Scattering, ETH Zurich and Paul Scherrer Institut, CH-5232 Villigen PSI

INTRODUCTION

The powder diffractometer DMC has been in operation for more than 20 years, first as a thermal neutron powder diffractometer at the reactor Saphir at PSI [1] and later as a cold neutron diffractometer for powder and crystal applications at SINQ [2]. The instrument is well accepted by the user community, which is clearly documented by both the overload factor of the instrument as well as the scientific output in terms of publications.

While monochromator and instrument electronics have been replaced when DMC was moved to SINQ, the main instrument from sample table to detector, including detector electronics, is basically in its original state. With 20 years of operation the guaranteed lifetime of the detector is highly exceeded and a damage of essential parts either of the detector or its electronics would lead to a temporary or final shut down of the instrument. Moreover, detector technique has highly developed since the mid-eighties and competition from modern diffractometers at other neutron centers is constantly growing.

Therefore, we plan a major upgrade of DMC, i.e. the replacement of the secondary instrument. The design of the new cold neutron diffractometer was motivated by clear goals:

- highest achievable intensity, resulting in a significant increase compared to the present DMC
- no decrease of resolution when compared to current DMC
- enable significantly improved sample environment conditions (e.g. high pressure, high magnetic fields)
- versatility, application to powder and single crystal diffraction, including pole figure measurement and texture analysis

The crucial point of the DMC upgrade is the large state-of-the-art detector. State-of-the-art means high efficiency through high gas

pressure, large covered angle range in the scattering plane as well as perpendicular to it and pseudo-2D detection of scattered neutrons to resolve the curvature of the Debye-Scherrer cones. This will be fulfilled with a large "banana-type" detector consisting of linearly position-sensitive counting wires. A new tool for instrument design that turned out to be very helpful is Monte Carlo ray-tracing simulation. With proper programming of the modules for the neutron source, neutron guide, monochromator, collimations and detector, we were able to reproduce the experimentally determined intensity relations and resolution functions of the present DMC. To optimize the design of the new detector, we performed similar model calculations for various dimensions, number of wires, heights etc. and determined the intensity gain and resolution functions. The final design represents the optimal solution in terms of intensity gain without loss of resolution, taking into account the available space for a new instrument. Unlike the present DMC, which was initially built for applications on a thermal beam tube, the upgraded instrument will be designed for and dedicated to the special needs of a cold neutron diffractometer at SINQ. The total intensity gain factor compared to present DMC will be up to 14, depending on wavelength and instrument configuration. More than one order of magnitude gain in intensity will open up totally new fields of research (small samples, small magnetic moments, high pressure, fast processes, in-situ experiments…). Moreover the new non-magnetic construction of detector housing and sample table will enable the use of high magnetic fields up to 15 Tesla.

High-quality diffraction data greatly depends on the technical solutions for the neutron detection. Similarly, it depends on proper data treatment to obtain a correct and aberration-free powder pattern by integrating the two-dimensional raw data. Following, algorithms for data integration and corrections are outlined.

PURPOSE

The next generation 2-D neutron powder detectors open a whole new set of possibilities as being able to collect data more quickly and efficiently. A further aspect that deserves full exploitation is the vertical position sensitivity (hereafter vertical will be the direction perpendicular to the average scattering plane). This additional information richness can be exploited – using appropriate algorithms – to correct for sample positioning aberrations and to eliminate the effect of the vertical aperture of the detector, integrating the pattern along the correct constant-diffraction angle curves on the detector surface. This leads, as we will show, to a dramatic improvement in the data quality.

The calibration of a neutron powder detector entails usually two phases:

(1) Vanadium calibration:

Calibration of the sensitivity of each pixel, normally repeated at short time intervals comprising several experiments (say, monthly).

(2) Standard calibration:

Calibration of the wavelength and the zero of the scattering angle, normally repeated at short time intervals comprising several experiments (say, monthly).

For a 2-D detector a third phase is envisaged:

(3) Geometric self-calibration:
Geometric aberration determination and self-correction, to be performed on each experimental dataset, in the data reduction phase.

This would replace and/or integrate the procedure of centering the sample with respect to the curvature center of the detector [3].

DESCRIPTION OF A 2-D DETECTOR

The detector has height H and angular aperture ζ_0 with curvature radius R. It contains N_v pixel in the vertical direction, each of height $h=H/N_v$. Similarly, there are N_t pixels in the tangential direction, each of width $\Delta r=R\,\Delta(2\theta)=R\,\zeta_0/N_t$. We shall identify pixels by a pair of indexes m, n, $m = 1\ldots N_t$, $n = 1\ldots N_v$. Pixel m, n corresponds to in-plane scattering angle $2\theta_m = 2\theta_0 + (m-1)\Delta(2\theta)$ (with respect to the ideal beam direction) and at vertical position $z_n = z_0+(n-1)h$. Note that the ideal sample position along z is set to $z_s = z_0+(N_v-1)h/2$. We will call ξ the adimensional coordinate $\xi = (z-z_s)/R$. After an exposure to scattered radiation from any sample, each pixel will have recorded a certain neutron count C_{mn} to which we immediately associate

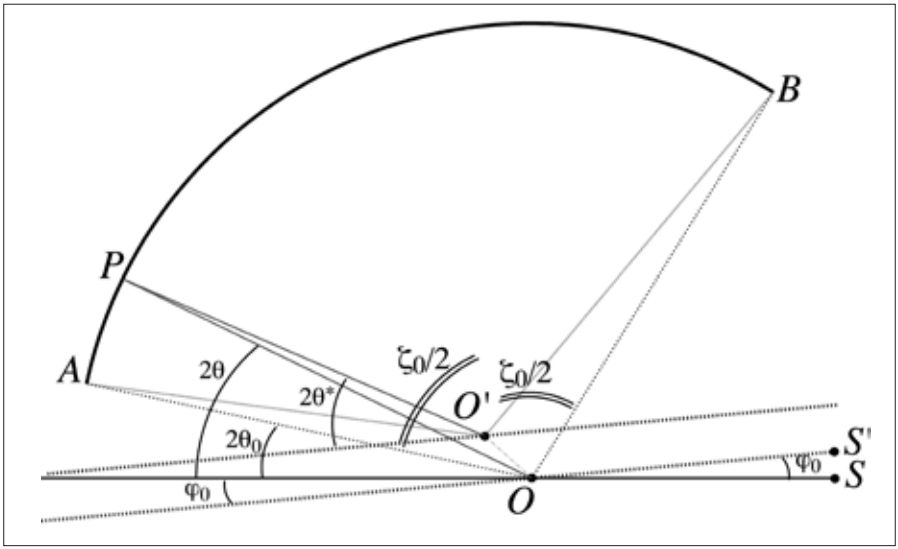

Fig. 1: A 2-D detector (diffraction plane projection). The detector surface is represented by arc *AB*. *O* is the ideal sample position, *S* the ideal position of the slit, *S'* and *O'* the real sample and slit positions, φ_0 the diffraction angle offset due to the slit misplacement. ζ_0 is the full detector aperture, *Oxyz* is a coordinate system with *z* orthogonal to the diffraction plane, *x* directed along the ideal incident beam direction and y orthogonal to it. $2\theta_0$ is the ideal in-plane diffraction angle corresponding to the first detector pixel. *P* is a detector pixel corresponding to the ideal in-plane diffraction angle 2θ and to the real in-plane diffraction angle $2\theta^*$. Dotted lines correspond to the incident beam.

Fig. 2 Simulated intensity on a 2-D detector surface. The detector aperture is 80° with radius R=1600mm and full height H=400mm; $2\theta_0$=10° (2θ increases towards the right). The surface is divided in N_t=800 and N_v=40 pixels. The simulation refers to a frequently used standard powder ($Na_2Al_2Ca_3F_{14}$, commonly named NAC) at a wavelength of 2.45Å, one of the most commonly used in the DMC wavelength range. Bright lines correspond to Bragg peaks. Note the prominent curvature at low scattering angles.

the Poisson-Cauchy standard deviation $s_{mn}=[C_{mn}+1]^{1/2}$. Now we will proceed by steps through the different phases of data elaboration that will lead us to obtain aberration-free one-dimensional powder patterns of high quality.

VANADIUM CALIBRATION OF A 2-D DETECTOR

Here the only difference to be remarked is that – even if all pixels are of constant area – unless they lie on the same *z* level of the sample, they are not orthogonal to the diffracted beam. The cosine of the angle between the *m,n*-th pixel normal and the diffracted beam is

$$\eta_{mn}=\left[1+\left(\frac{z_n-z_s}{R}\right)^2\right]^{-1/2}=\left[1+\left(\frac{(n-(N_v+1)/2)h}{R}\right)^2\right]^{-1/2}=\frac{1}{\sqrt{\xi_n^2+1}}.$$

If the neutron count with the vanadium miscut crystal (a uniform spherical scatterer) is C_{mn}, the sensitivity correction factor will be $\nu_{mn}=<C/\eta>/[C_{mn}/\eta_{mn}]$, where $<C/\eta>$ is the weighted average over all pixels of C_{mn}/η_{mn}:

$$<C/\eta>=\frac{\sum_{mn}\frac{C_{mn}\eta_{mn}}{C_{mn}+1}}{\sum_{mn}\frac{\eta_{mn}^2}{C_{mn}+1}}$$

SCATTERING ANGLE ON THE DETECTOR SURFACE

With 1-D detectors the scattering angle – the angle between the incoming and the diffracted beam – is just the in-plane angle 2θ as seen in Fig. 1. On a 2-D detector, for each point on the surface we have to take into account the off-plane z shifts $\Delta z=R\xi$ with respect to the sample position.

Therefore the planar scattering angle 2θ has to be replaced by the true scattering angle $2\theta^*$ (function also of ξ) given by

$$2\theta^* = \arccos\left(\eta\cos(2\theta)\right)$$

where we recall that $\eta = 1/[\xi^2+1]^{1/2}$.

LORENTZ FACTOR FOR A 2-D DETECTOR

The Lorentz factor for powder diffraction contains one factor which weights the part of the scattered wave that is actually seen by the detector, and this is the only one that is going to be changed.

The classical powder Lorentz factor is defined – within a proportionality constant – as

$$\mathcal{L}(2\theta) = \frac{1}{\sin(2\theta)\sin(\theta)} = \mathcal{C}(2\theta)\mathcal{S}(2\theta)$$

where the first factor *(cone factor) C* depends on the detector geometry, the second, *S*, depends only on the sample. For 1-D detectors – where all pixels are centered in the scattering (horizontal) plane – it is classically (within a proportionality factor)

$$\mathcal{C}(2\theta) = \frac{1}{\sin(2\theta)}; \qquad \mathcal{S}(2\theta) = \frac{P(\theta)}{\sin(\theta)}$$

where *P* depends on the incoming beam polarization and is normally 1 for unpolarized beams. For a pixel on a 2-D detector, these factors both change slightly. Without going into the most complex details, for *S* it suffices to substitute the planar half scattering angle θ by the true half scattering angle θ^* (see the former section). For *C* instead it turns out that the same expression can be used, leaving the planar half scattering angle θ. Formally,

$$\mathcal{C}(2\theta,\xi) = \frac{1}{\sin(2\theta)}; \qquad \mathcal{S}(2\theta,\xi) = \frac{P(\theta^*)}{\sin(\theta^*)}$$

where the dependence on ξ is only through θ^*.

SAMPLE-DEPENDENT ABERRATIONS

We consider here aberrations depending on the sample being not in the ideal position *O* but instead in

$$O' = R\left(\rho\cos(\beta), \rho\sin(\beta), \delta_z\right)$$

with respect to the *xyz* frame (see Fig. 1). We shall deal hereafter with the standardless determination of ρ, β, δ_z and their usage in order to correctly integrate the diffraction pattern along the (deformed) constant-true-scattering-angle curves on the detector surface. Standardless means that the determination of ρ, β, δ_z can be performed based only on some very general properties of the powder diffraction pattern of an average powder sample. It is useful if the pattern shows several Bragg peaks, but the structural information is not used, making the computation much faster and allowing it to be performed at the data reduction stage (prior to structural analysis). Nevertheless, the wavelength has to be determined using a standard powder, as customary. The standard is also used for determining the zero of the scattering angle φ_0. A further correction due to sample displacements ρ, β might be necessary and it needs to be performed on the data during the structural analysis, but the generality of structure analysis program allows for this.

SCATTERING ANGLE ON THE DETECTOR SURFACE IN THE PRESENCE OF SAMPLE DISPLACEMENTS

The general expression of the true scattering angle is more complex than the one above reported, valid in the ideal case. We shall split the task in two phases, because the coupling between the vertical and the in-plane displacements is negligible. Therefore we will consider first the case when only vertical aberration is present ($\rho = 0$, $\delta_z \neq 0$). Then we will present the case of planar aberration only ($\rho \neq 0$, $\delta_z = 0$). Finally we shall present the procedures able to determine and correct the vertical aberration and the planar one (separately), so that the general case can be neglected.

VERTICAL ABERRATION

The expression of the true scattering angle in the presence of a vertical sample displacement $\boldsymbol{\delta}_z = R\,\delta_z$ is trivial. In fact, the z-dependence of the true scattering angle is all through the relative distance from the plane of the sample. Therefore it suffices to replace ξ by $\xi' = \xi - \delta_z$ and η by $\eta' = 1/[(\xi')^2+1]^{1/2}$. Once δ_z is known, a change of origin is enough to correct for it. The true diffraction angle will be then

$$2\theta^* = \arccos\left(\eta' \cos(2\theta)\right)$$

Inverting with respect to the planar diffraction angle, we obtain

$$2\theta = \arccos\left(\frac{\cos(2\theta^*)}{\eta'}\right)$$

This is important because it allows us to draw the constant-true-scattering-angle curves on the detector surface. Drawing the curves is important because it allows us to integrate the pattern along the constant-true-scattering-angle lines. For integrating the discrete intensity distribution on the detector surface we need to interpolate the observed intensity (already corrected for pixel sensitivity – according to the vanadium calibration – and for the Lorentz factor) between data points. The simplest way to do this is bilinear interpolation (see [4]). More complex interpolation methods (e.g. bicubic) give better results but they are also more time-consuming. The detailed evaluation of this and other advanced aspects will be the argument of a forthcoming paper. Hereafter we shall present results obtained by bilinear interpolation. Note that the resulting integrated intensities – corresponding to a selected $2\theta^*$ grid – will always be calculated as linear combinations of a certain number of pixel intensities. Therefore the standard deviations will also be easily determined using the well-known weighted-average method.

At this point we have the possibility to calculate an integrated 1-D pattern I_n, $n=1\ldots N_{obs}$, and the relevant standard deviations σ_n, for every arbitrarily chosen value of δ_z. Now we can define (see also [5]) two functions of the pattern, the sharpness

$$\mathrm{Sh} = \sum_{n=2}^{N_{obs}} \frac{I_n - I_{n-1}}{\sigma_n^2 + \sigma_{n-1}^2}$$

or the symmetry

$$\mathrm{Sy} = \sum_{n=1}^{N_{obs}} \frac{(I_n^+ - I_n^-)^2}{(\sigma_n^+)^2 + (\sigma_n^-)^2}$$

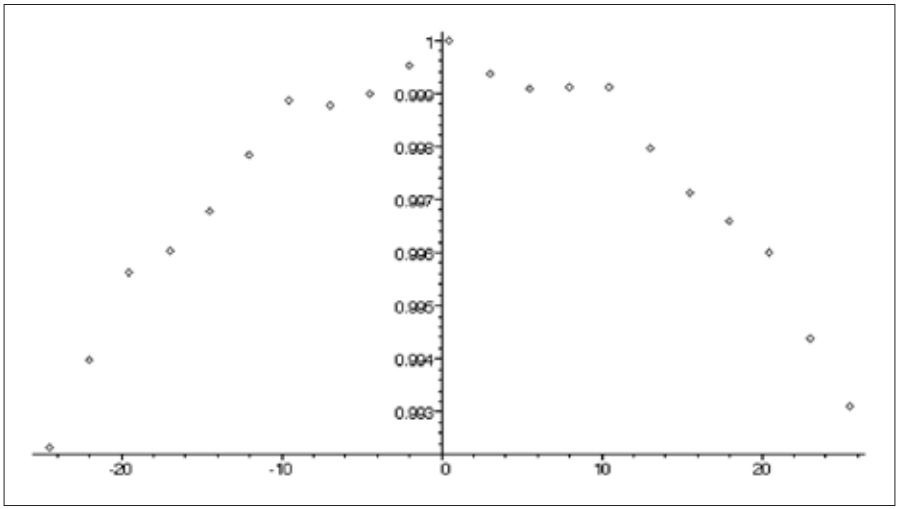

Fig. 3 Sharpness function plot (a.u.) around the true position. Abscissa is the vertical sample displacement (mm) with respect to the true value. The sample-detector distance is R=1600mm, so a displacement of 10mm corresponds to $\xi = 0.00625$ and $\eta = 0.9999805$. A simple 1-D scan can find a maximum <1 second. Kinks are due to the simple (bilinear) interpolation algorithm used.

where I^+ and I^- (as well as the related σ) are obtained by partially integrating for $\xi'>0$ or <0, respectively. As **Sh** and **Sy** are functions of δ_z only, one can proceed assuming that the actual value of δ_z will bet the one that maximizes **Sh** – or minimizes **Sy**. Our first tests demonstrate (a bit surprisingly) that **Sh** is superior in performance and accuracy. This is good news because the sharpness is faster to compute and it is supposed to be more robust with respect to special sample features (texture). A plot of the behaviour of **Sh** around the true value is shown in Fig.3.

PLANAR ABERRATION

The expression of the true scattering angle in the presence of a planar sample displacement is a bit more involved. Firstly, in order to simplify the treatment, we shall neglect hereafter the effects of the zero of the scattering angle φ_0. In other words, we shall assume that the incident beam on the sample is directed to $2\theta=0$. In fact, both φ_0 and ρ (the magnitude of the horizontal sample off-center shift divided by the sample-detector distance) are quite small and it can be shown that the distortion effect due to $\varphi_0 \neq 0$ is of second order in φ_0 and ρ and therefore negligible. On the other side, as mentioned, all available data analysis software can cope with a small scattering angle bias.

Assuming then that the beam is in the ideal direction but the sample is shifted by ($\rho \cos\beta$, $\rho \sin\beta$, 0) in the *xy* plane we obtain the following expression for the true scattering angle as a function of the ideal planar scat-

tering angle 2θ, of the vertical coordinate (here encoded into η) and of ρ, β:

$$\cos(2\theta^*) = \frac{\eta\left(\cos(2\theta) - \rho\cos(\beta)\right)}{\sqrt{1 + \rho\eta^2\left(\rho - 2\cos(2\theta - \beta)\right)}}$$

In reality we would need the inverse expression – yielding 2θ as a function of $2\theta^*$, ρ, β, η. There is an analytical expression that can be found by substituting

$$2\theta = 2\arctan(t)$$

into the former and solving with respect to *t* the resulting 4^{th} degree equation. However, because the resulting expressions are quite involved and furthermore numerical solution is competitive with analytical solution for this inversion, we shall simply denote the inverse as

$$2\theta = \Psi(2\theta^*, \eta; \rho, \beta)$$

Now, given any trial value for the ρ, β pair, we can construct the constant-true-scattering-angle curves on the detector surface and integrate the signal along them. Again we can follow the principle of maximum sharpness – already introduced in the former sections – and accept as true the ρ, β pair that maximizes the sharpness function **Sh**. An example of the **Sh** surface around the true value of the sample position is given in Fig. 4.

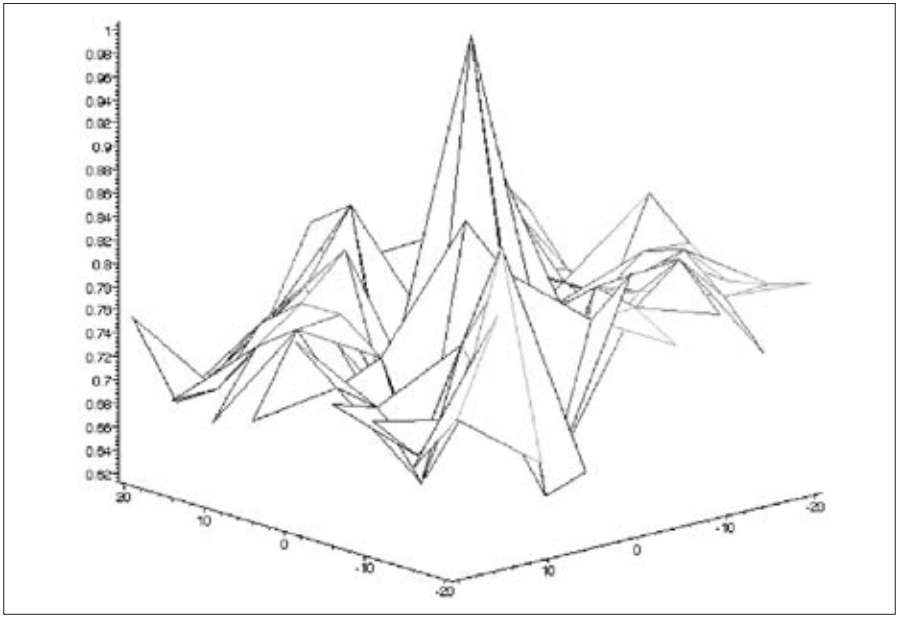

Fig. 4 Sharpness function plot (a.u.) around the true sample position in the horizontal plane. The plane coordinates are x-ρ cosβ and y-ρ sinβ, or the cartesian displacement components (mm) from the ideal sample position in the horizontal plane. Note the sharp maximum in the center. A simple grid-scan algorithm can be used to find the maximum, with a CPU-time requirement in the order of few seconds. Again, the surface roughness is due to the low-level (bilinear) interpolation here used. Roughness is just an aesthetic nuisance as it does not prejudice the effectiveness.

FINAL DATA REDUCTION

The final data reduction step is the integration in a 1-D powder pattern. This task has been previously described. At this point sample displacement parameters have been determined and aberration-compensated constant-true-diffraction-angle curves can be drawn on the detector surface, in order to obtain the most faithful integration of the pattern, without detector aberrations. The Lorentz factor is properly taken into account during the integration process, and depending on the data analysis program requirements, output data can either be Lorentz factor-free or include a properly calculated Lorentz factor for a 1-D pattern.

The advantages of integrating along the curved constant-true-diffraction-angle paths on the detector surface with respect to crudely integrating along the vertical direction (summing pixel columns) are evident in Fig. 5, where the same pattern (see Fig. 2) has been integrated with the two methods. Peak profile asymmetric broadening and anisotropic shifts – artifacts of the vertical integration – are visibly corrected for.

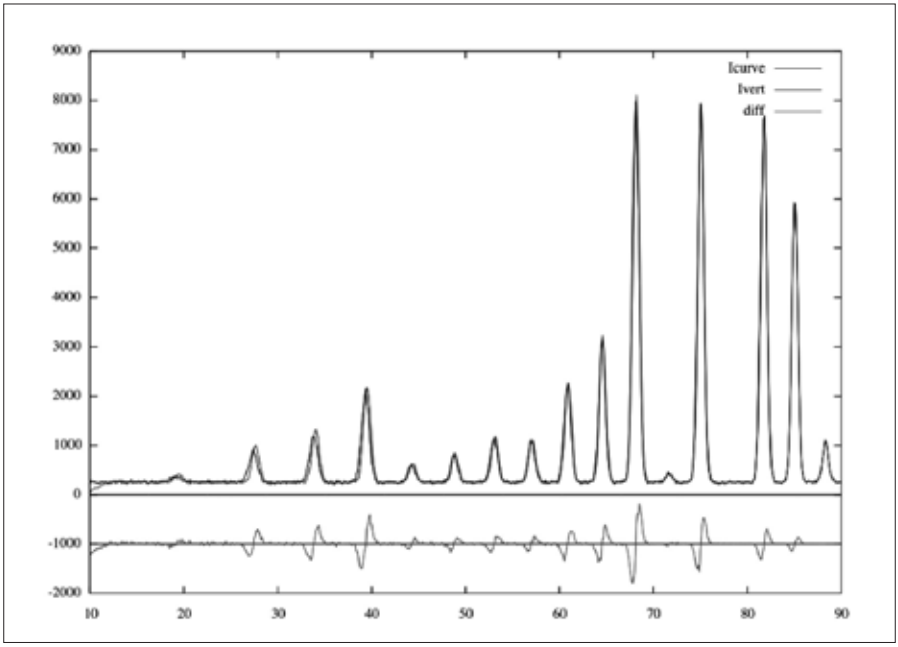

Fig. 5 Exemplification of the advantages of integrating a 2-D pattern (see Fig. 2) along the correct curved constant-true-diffraction-angle paths or along vertical pixel columns (as in a classical 1-D detector). The difference plot (below) is on the same scale. Apart from the sharper peak shape, the curved-integration is able to correct a disturbing effect of anisotropic peak shift present in the verically integrated pattern.

SUMMARY AND CONCLUSIONS

The forthcoming updgrade of the DMC neutron powder diffractometer has been illustrated. The new 2-D detector project will open a whole new set of possibilities for more advanced experiments. In order to fully exploit the new detector's capabilities, the data collection and reduction software shall be also innovated in the way to a) self-correct geometric aberrations due to sample misplacement, b) integrate the pattern to 1-D in the most faithful possible way.

In this way, we plan to keep the DMC diffractometer at the cutting edge of the scientific research and to satisfy the requests of its broad Swiss and international user community.

REFERENCES

[1] J. Schefer, P. Fischer, H. Heer, A. Isacson, M. Koch and R. Thut, *Nuclear Instruments and Methods in Physics Research A* **288**, 477-485 (1990)

[2] P. Fischer, L. Keller, J. Schefer and J. Kohlbrecher, *Neutron News* **11**, No. 3, 19-21 (2000)

[3] L. Cranswick, Oral contribution, EPDIC10 conference (Geneva, Sept. 2006) http://www.sgk-sscr.ch/EPDIC10/Abstracts/Instrumentation/Oral/CranswickNo76.doc

[4] W.H. Press, B.P. Flannery, S.A. Teukolsky, W.T. Vetterling, *Numerical Recipes in Fortran 77, 2nd Ed.,* Cambridge University Press: Cambridge, chap. 3 (1992)

[5] A. Cervellino, C. Giannini, A. Guagliardi and M. Ladisa, *J. Appl. Cryst.* **39**, 745-748 (2006)

// MEGAPIE at SINQ – the First Liquid Metal Target Driven by a Megawatt Class Proton Beam //

W. Wagner, F. Gröschel, K. Thomsen and H. Heyck
Paul Scherrer Institut, 5232 Villigen PSI, Switzerland

The lead-bismuth liquid metal target MEGAPIE (MEGAwatt PIlot Experiment) was operated at the Swiss Spallation Neutron Source SINQ starting mid-August 2006, for a scheduled irradiation period until December 2006. The continuous (51 MHz) 590 MeV proton beam hitting the target reaches routinely an average current of ~1300 µA, corresponding to a beam power 0.77 MW. This article illustrates the main features of the target and the ancillary systems specially needed for the liquid metal target operation. Further, the operational experiences made with this target during start-up and routine operation are summarized, besides the general performance highlighting the performance of new beam and target safety devices, and last but not least the neutronic performance in relation to the previously operated solid lead target.

INTRODUCTION

SINQ, the Swiss spallation neutron source, is driven by PSI´s 590 MeV proton accelerator. Receiving a stable proton current of 1.3 mA, SINQ is the presently most powerful accelerator driven facility worldwide. Besides the primary designation of SINQ to serve as user facility for neutron scattering and neutron imaging, PSI seeks to play a leading role in the development of the facility, focusing to spallation targets and materials research for high-dose radiation environments. Serving these activities, SINQ has established several projects, the most prominent one being MEGAPIE (Megawatt Pilot Experiment), a joint initiative by six European research institutions, plus EU, JEAE (Japan), DOE (USA), and KAERI (Korea) to design, built, operate and explore a liquid lead-bismuth spallation target for 1 MW of beam power [1]. Such a target is under consideration for various concepts of accelerator driven systems (ADS) to be used

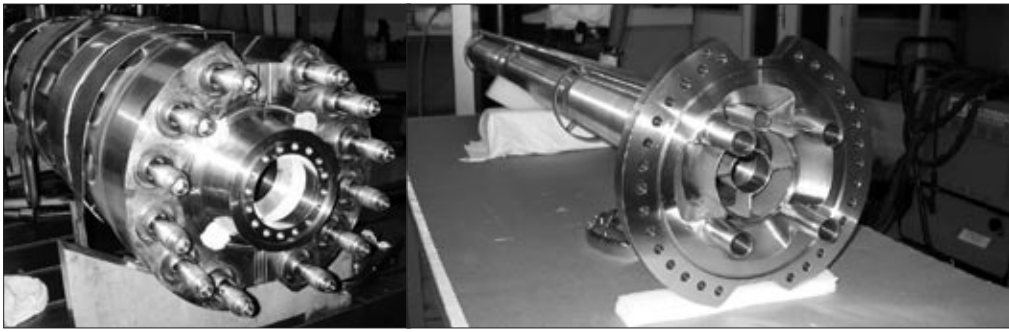

Fig. 1: Two major target components prior to integration: the 12-pin heat exchanger (left) and the central flow guide tube.

in transmutation of nuclear waste and other applications worldwide. The goal of this experiment is to explore the conditions under which such a target system can be licensed, to accrue relevant materials data for a design data base for liquid metal targets, to gain experience in operating such a system under realistic beam conditions, and to ascertain the neutronic performance of such a target for the use in SINQ and other (future) accelerator driven neutron sources.

THE MEGAPIE TARGET

In shape and external dimensions, the MEGAPIE target has to match the given opening in the target block shielding, demanding a slim, about 5 m high structure [2]. In its interior, it is completely different as compared to the normal solid 'lead-cannelloni' target of SINQ: The MEGAPIE target houses about 1 ton of liquid lead bismuth eutectic (LBE, melting point at 125 °C) in a steel container, closed-end by a hemispherical beam window at the bottom. The main features inside are two electromagnetic pumps for forced circulation of the LBE, a flow guide tube inserted into the lower liquid metal container to separate the annular LBE down-flow from the central up-flow, and twelve heat exchanger pins for removing the energy deposited by the beam and/or keeping the target at temperature when the beam is off. Further, the target is equipped with a variety of instrumentation, mostly thermocouples, for operational control, or serving safety features or experimental observation. Figure 1 shows two of the major target components, i.e. the 12-pin heat exchanger (lower right) and the central flow guide tube. Figure 2 shows the fully assembled MEGAPIE target lifted before inserting it into the SINQ operation position.

ANCILLARY SYSTEMS

The MEGAPIE ancillary systems directly necessary for the target operation are the heat removal system (HRS), the cover gas system (CGS), the insulation gas system (IGS) and the fill and drain system (F&D).

Fig. 2:
The fully assembled MEGAPIE target before inserting it into the SINQ operation position.

The HRS [3] consists of two subsystems: an intermediate cooling loop with oil Diphyl THT as cooling medium, connected to the heat exchanger pins in the target, and a back-cooling water loop (WCL). The oil loop, operating between 160 °C and 230 °C, is primarily necessary to remove the about 0.6 Megawatt of heat load deposited in the LBE by the proton beam. As a second function it must also be capable to manage a controlled hot-standby operation after beam trips or scheduled beam interruptions to prevent freezing of the target.

The CGS [4] must handle the volatile radioactive inventory of spallation products released from the LBE in the target. Handling of radioactive gases and volatiles imposes stringent requirements on safe and remote operation, on retention of radioactivity, like second containment and tightness, and on shielding.

The IGS [5] fills the volume between the inner hot part of the target and the outer cold hull by an insulating gas. Besides its function as thermal barrier it must safely cope with the potential incident of cooling water entering the insulation gap and getting into contact with the hot interior of the target.

The F&D system is needed to allow filling and draining of liquid LBE into or out of the target, respectively. Figure 3 shows a view from top into the target head enclosure chamber TKE (situation of April 2006). The target head is in the centre, still without the cables connected which are in preparation in the rear, the oil loop of the HRS is at the right, the CGS in the left rear corner, and the F&D system at the left.

The initial baseline for the F&D system required draining of activated LBE from the target after the operation period. A detailed design for that was elaborated; however, the draining option was recognised to bear considerable risks, immediate ones for accessing the TKE and more general ones related to licensing. As well, it had required considerable extra expenditure in the technical realization. Viewing these difficulties the decision was taken to abandon the initial concept in favour of only inactive draining and final freezing of the LBE in the target after completion of the irradiation experiment [6].

MEGAPIE IRRADIATION START-UP

The first beam on Megapie was received on Aug. 14, 2006, closely watched by the operational team and prominent guests in the SINQ control room, and documented in Figure

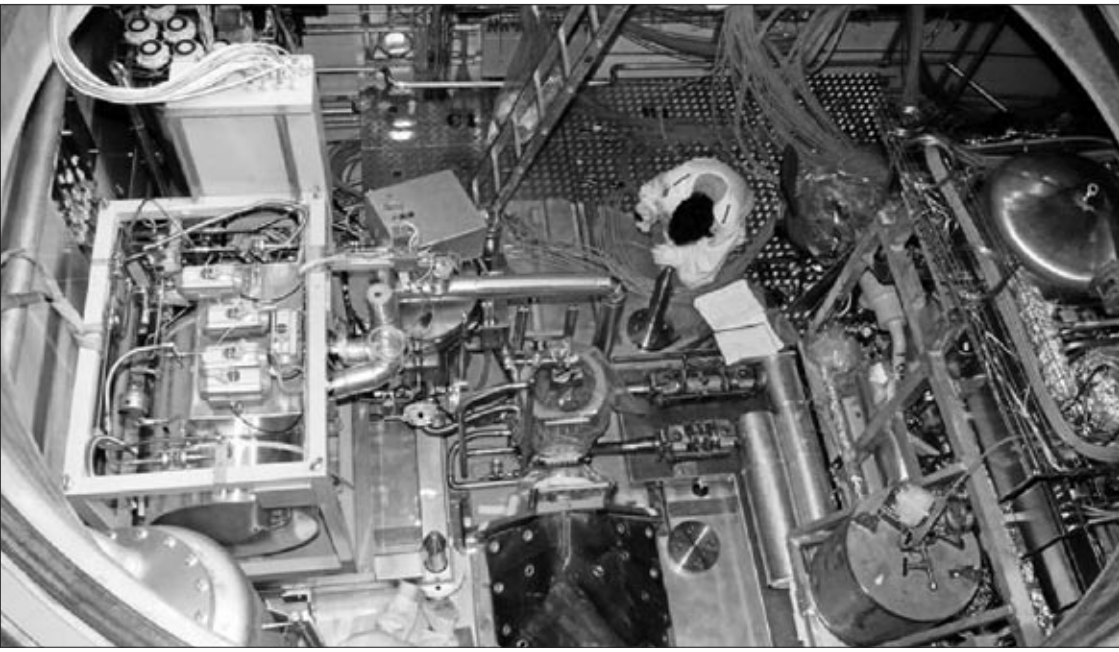

Fig. 3: View into the target head enclosure chamber TKE which is located on top of the SINQ main shielding block (situation of April 2006). The target head is in the centre, still without the cables connected which are in preparation in the rear, the oil loop of the HRS is at the right, the F&D system at the left, and the CGS in the left rear corner (partly hidden behind the connector box of the F&D).

4. At a relatively stable and constant beam current of 40 μA, which corresponds to about 25 kW of beam power, the target accumulated a total charge of 60 μAh in this first phase. The second phase of the start-up procedure was successfully accomplished the following day, where the power was stepwise increased to 150 kW (250 μA proton current). The corresponding beam history is shown in Figure 5. The goal of this phase was to check and verify the response of the heat removal system at power conditions comparable to those used when operated out of beam at the test stand in the autumn of 2005. The third and final phase of the start-up procedure was successfully accomplished on the 17th of

Fig. 4: First beam on Megapie, closely watched by the operational team and prominent guests (not all shown) in the SINQ control room: from left, a French colleague from CEA observing fission chamber reactions, Stefan Joray pointing to the screen, Sergej Dementjev, Kurt Clausen and Knud Thomsen.

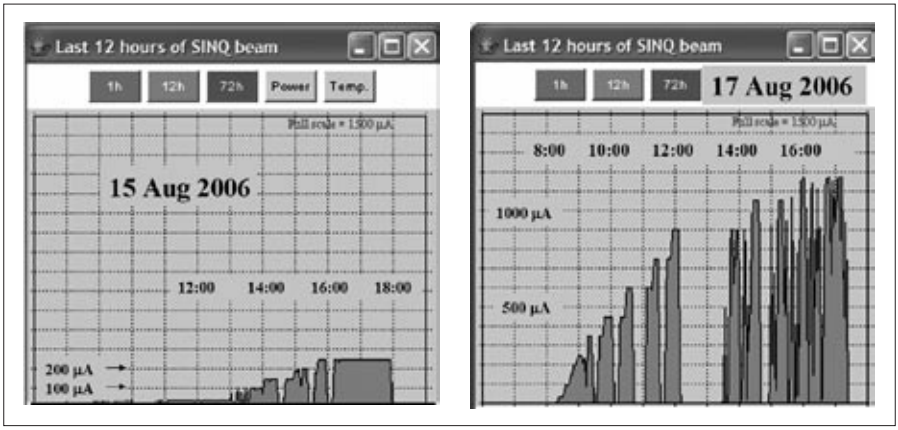

Fig. 5: Beam history during the second phase of the start-up procedure (Aug. 15) where the power was stepwise increased to 150 kW, and the third phase (Aug. 17) where the beam was ramped-up to full power. Most of the erratic beam behaviour was intentional.

August, when the power was stepwise increased to 700 kW (1200 µA proton current). The second graph of Figure 5 shows the beam history during the ramp-up phase. At each power level the beam was interrupted after some 10 minutes with a stable proton beam, to verify the predicted temperature transients in the target. Most of the erratic beam behaviour was thus intentional.

MEGAPIE IN USER OPERATION

With MEGAPIE, normal user operation was started on August 21st around 8:30 a.m., and was continued until the normal annual winter shut-down starting on December 21st, 2006. The first 12 hours of proton beam is seen in Figure 6. Since then SINQ with the MEGAPIE target was operating routinely and reliably. Meanwhile the goal current of 1350 µA has been reached. The statistics of weekly accumulated proton charge on SINQ is illustrated in Figure 7, distinguishing charge delivered by the accelerator and charge accepted by SINQ. The ratio of both defines the availability of SINQ which, except for the starting week, was at satisfactory 95%. The total proton charge accumulated at the end of week 49 was 2.54 Ah.

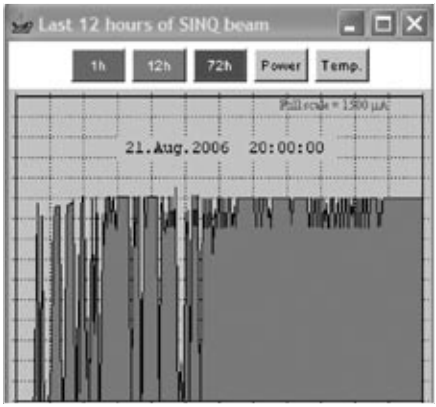

Fig. 6: The first 12 hours of proton beam when normal user operation had started on August 21st

During the entire MEGAPIE irradiation experiment the target behaviour was found excellent, both during stable operation and during transients due to beam trips and more extended beam interrupts. The temperature distributions and -transients were as expected, very close to predictions. The electromagnetic pumps operated stable and reliably, without any indication of degradation. For the main MEGAPIE ancillary systems directly connected to the target, i.e. heat removal system (HRS), the cover gas system (CGS), and the insulation gas system (IGS), the experience is very positive, as well. All in all, the MEGAPIE systems worked reliably according to specifications, exceeding our rather cautious expectations.

NEW PROTON BEAM SAFETY DEVICES

For its safe operation a sufficiently broad footprint of the incident proton beam on the SINQ target is mandatory. If for any reason the protons were not scattered sufficiently in an upstream target (Target E) their footprint on the SINQ target could shrink leading to a rise in the maximum density of the beam by a factor of 25. At the resulting high current density it would take only 170 ms until a hole is burned through both the liquid metal container inside the target and the lower target enclosure. The liquid metal would spill into the beam line and into the catcher vertically below the SINQ target. Such a failure would result in an extended shut down period for SINQ.

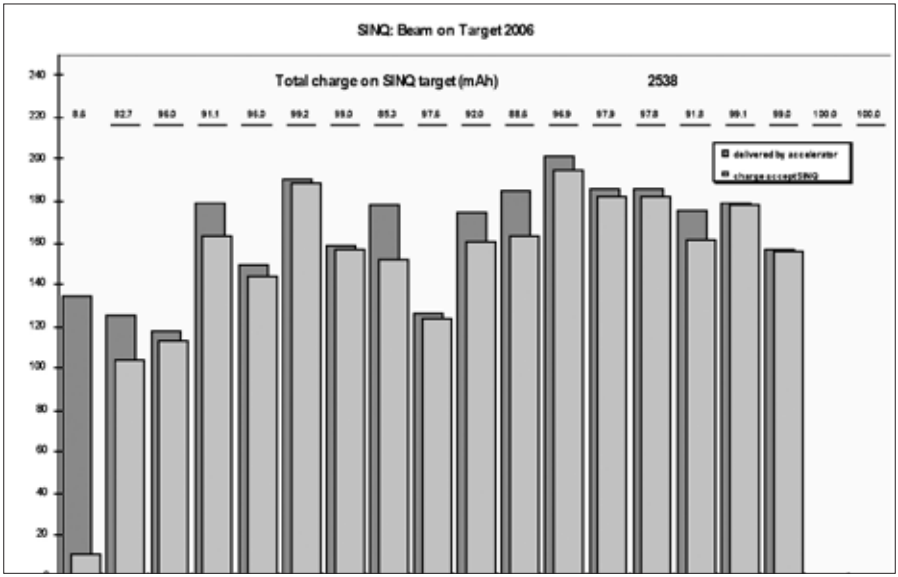

Fig. 7: Statistics of weekly accumulated proton charge on SINQ during MEGAPIE operation. The availability of SINQ, even with the complex MEGAPIE systems and various additional beam interrupt channels, was at the satisfactory level of ~95% .

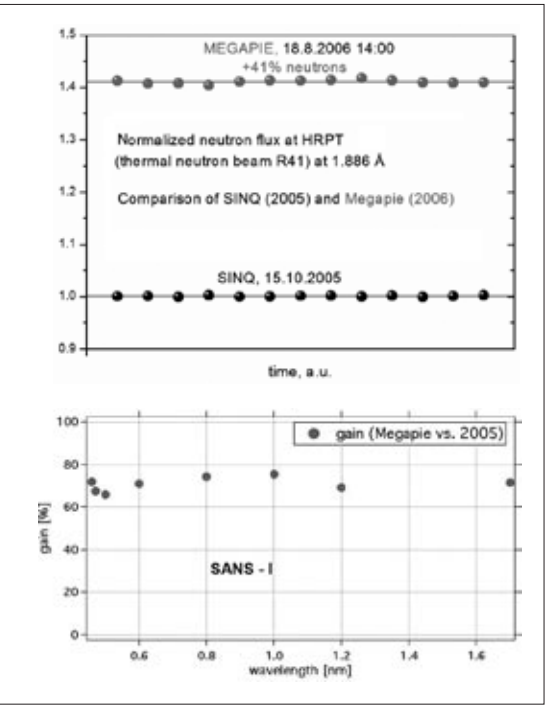

Fig. 8: Neutron flux increase by MEGAPIE in relation to the standard steel-lead cannelloni target, measured during the start-up phase of MEGAPIE: the powder diffractometer HRPT at the thermal beam port reported a flux increase of 41%, the SANS 1 instrument at the cold guide around 70%. Meanwhile gold foil activation measurements have confirmed flux increases between 80 and 85% at both, a thermal beam port (NEUTRA) and a cold beam port (ICON), and 70% at sector 80 (thermal water scatterer).

In order to prevent an insufficiently scattered beam from reaching the SINQ target three independent safety systems have been installed: a dedicated current monitoring system, a beam collimating slit and a novel beam diagnostic device named VIMOS [7]. The latter monitors the correct glowing of a tungsten mesh closely in front of the liquid metal target. All these systems have to meet the basic requirement to switch off the beam within 100 ms when 10 % of the protons by-pass Target E (corresponding to an increase in peak intensity by a factor of two). In an extensive collaboration amongst different groups at PSI the new safety devices have been installed. Early in the ramp-up phase as well as during routine operation their proper functioning has been verified.

NEUTRONIC PERFORMANCE OF MEGAPIE

During the start-up phases, several neutronic measurements were performed, i.e. measurements of delayed neutrons in the target head area, Bonner spheres and chopper measurements for spectral resolution at the ICON beamport, fission chamber measurements from inside the target and neutron flux measurements inside the D_2O Moderator and at selected instruments and beam ports. The neutron fluxes of MEGAPIE in relation to the previously operated solid lead target were of particular interest. Based on earlier Monte Carlo simulations the liquid metal target was expected to provide a 40% increase in neutron flux (at identical current). Initial measurements at selected instruments confirmed an increase in neutron flux which at first glance was met with some scepticism: While the powder diffractometer HRPT at the thermal beam port reported 41%, very close to the prediction, the SANS-I instrument at the cold guide quoted a flux increase as high as 70 to

80 % (see Figure 8). Meanwhile gold foil activation measurements have confirmed flux increases between 80 and 85% at both, a thermal beam port (NEUTRA) and a cold beam port (ICON), and 70% at sector 80 (thermal water scatterer). Revised calculations with more detailed target and moderator geometry reproduce these results.

REFERENCES

[1] G. S. Bauer, M. Salvatores, G. Heusener, J. Nucl. Mater. 296 (2001) 17

[2] F. Gröschel, A. Cadiou, S. Dementjev, M. Dubs, C. Fazio, T. Kirchner, Ch. Latge, P. Ming, K. Thomsen and W. Wagner, The MEGAPIE Project Status Update – High Power Liquid Metal Spallation Target, Proc. ICANS-XVII , International Collaboration on Advanced Neutron Sources, Santa Fe, NM, LA-UR-06-3904 (2006) 590

[3] G. Corsini, M. Dubs, B. Sigg, W. Wagner, Heat Removal System: Final Update of Concept and Detail Design, Dimensional and Functional Issues, Proc. 4th MEGAPIE Technical Review Meeting, FZKA 6876 (2003) 34

[4] W. Wagner, F. Groeschel, G. Corsini, Cover Gas System: Updated Boundary C onditions and Current Concept, Proc. 4th MEGAPIE Technical Review Meeting, FZKA 6876 (2003) 40

[5] W. Wagner, J. Welte, S. Joray, B. Sigg, Insulation Gas System of MEGAPIE: A Concept Update, Proc. 4th MEGAPIE Technical Review Meeting, FZKA 6876 (2003) 52

[6] W. Wagner, P. Turroni, P.Agostini, K. Thomsen, E. Wagner, J. Welte, Fill and Drain and Freezing: System Modifications for Merely non-active Draining, Proc. 4th MEGAPIE Technical Review Meeting, FZKA 6876 (2003) 46

[7] K. Thomsen, VIMOS, a Novel Visual Device for Near-Target Beam Diagnostics, Proc. ICANS-XVII , International Collaboration on Advanced Neutron Sources, Santa Fe, NM, LA-UR-06-3904 (2006) 374

// Announcements //

SGN/SSDN MEMBERS

The Swiss Neutron Scattering Society welcomes the following new members:

– Justin Hoppler, University of Fribourg, Switzerland
– Suresh Chathot, University of Göttingen, Germany
– Rajashekhara Shabadi, University of Lille, France

Presently the SGN has 200 members. Online registration for new members of our society is available from the SGN website: http://sgn.web.psi.ch

PETER ALLENSPACH NEW ENSA CHAIRMAN

On the occasion of the recent meeting of the 'European Neutron Scattering Association ENSA' in October 2006 the President of the 'Swiss Neutron Scattering Society' Peter Allenspach (Paul Scherrer Institut, NUM department) was elected as new ENSA chairman. The term of office is two years.

OPEN POSITIONS AT ILL

To check the open positions at ILL please have a look at the ILL-website: http://www.ill.fr/jobs.html.

NEWS FROM PSI USER OFFICE

2006 was a very encouraging year regarding the submission of new SINQ proposals: Thanks to the very active user community totally 328 new proposals were submitted at the two deadlines in May and November. That number exceeds the previous record of 213 in the year 2004 by more than 50%!

As before the SINQ user community is very international: The proposals for cycle I/07 originate from 22 different countries, one third was submitted by authors with a Swiss affiliation (see figures below).

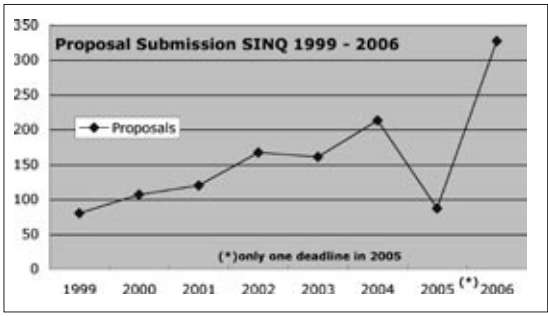

Submitted Proposals since 1999, (*): in 2005 only one call for proposals was opened instead of two (extended MEGAPIE shutdown).

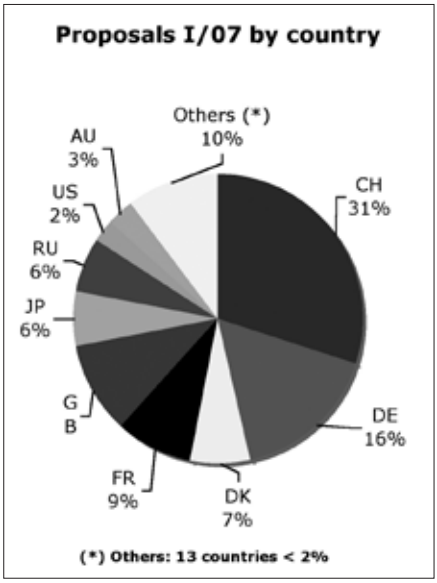

Geographical distribution of new SINQ proposals (cycle I/07).

SINQ USERS' MEETING 2007

The 2007-SINQ users' meeting will be organized as a special session during the ECNS conference to take place in Lund, June 25-29, 2007:

http://www.ecns2007.org

The users' meeting will consist of one session (half a day) with oral presentations, which will NOT overlap with plenary ECNS sessions. In conjunction with the ECNS program committee some abstracts submitted to ECNS and containing SINQ results will be selected for oral presentations at the SINQ users' meeting.

Therefore, in order to facilitate the organization, and if your work involves SINQ, we ask you to send a copy (MS word or pdf) of your submitted abstract to sinq@psi.ch with the mention „SINQ users meeting" in the headline.

The ECNS deadline for abstract submission is February 5, 2007.

Limited funds covering the registration fee and travel (economy class) will be available for the selected speakers of the SINQ users' meeting.

In addition, the annual meeting of the Swiss Neutron Scattering Society SGN (http://sgn.web.psi.ch) will be organized in connection with the SINQ users' meeting.

10TH ANNIVERSARY OF SINQ

In summer 1997 the first user experiments were performed at SINQ. Ten years and approximately 2000 experiments later the Swiss neutron source has become a real success. The 10th anniversary of SINQ will be celebrated in a special occasion at PSI on **September 21, 2007.** More information will be published on the SINQ webpage: http://sinq.web.psi.ch

// The 2007 Walter Hälg Prize of the European Neutron Scattering Association //

THE WALTER HÄLG PRIZE

The prize was made available to the European Neutron Scattering Association (ENSA) by a donation from Professor Walter Hälg who is the founder of neutron scattering in Switzerland. The Prize is awarded biennially to a European scientist for outstanding, coherent work in neutron scattering with long-term impact on scientific and/or technical neutron scattering applications. The previous Prize winners were F. Mezei (1999), J. Brown (2001), R. Cowley (2003), A. Furrer and H.U. Güdel (2005). The fifth award of the Prize (10'000 CHF) is to be made at a special ceremony and session at the 4th European Conference on Neutron Scattering (ECNS 2007), 25–29 June 2007, Lund, Sweden. Information on previous laureates are available on the ENSA web-site (http://neutron.neutron-eu.net/n_ensa).

SELECTION COMMITTEE

Nominations for the prize will be considered by a Selection Committee which consists of authorities representing the major scientific disciplines. It includes acknowledged experts both in neutron scattering and from outside the neutron scattering community. Membership in the Selection Committee is obtained by invitation extended by the ENSA Committee.

CALL FOR NOMINATIONS

Nominations for the 2007 Walter Hälg Prize of the European Neutron Scattering Association (ENSA) may be submitted by European scientists as individuals or on behalf of a Division, Section or Group. To establish a high standard it is necessary that the Committee receive

proposals which represent the breadth and strength of European neutron scattering.

Nominations should include the motivation for the award, a brief curriculum vitae of the nominee and a short list of major publications. Letters of support from authorities in the field which outline the importance of the work would also be helpful. Nominations for the Prize will be treated in confidence and although they will be acknowledged there will be no further communication. Previous nominations have to be up-dated and resubmitted.

DEADLINE

Nominations should be sent before **2 March 2007** to the Chairman of the Selection Committee, preferably by electronic mail in pdf format:

Dr. Peter Allenspach, ENSA Chairman
Paul Scherrer Institut
CH-5232 Villigen PSI, Switzerland
Phone: +41 56 310 2527
Fax: +41 56 310 2939
E-mail: peter.allenspach@psi.ch

Erwin Felix Lewy Bertaut prize of European Crystallographic Association and European Neutron Scattering Association (ECA-ENSA)

The European Crystallographic Association (ECA) and the European Neutron Scattering Association (ENSA) announce the creation of a prize in honour of the late Erwin Felix Lewy Bertaut, in memory of his scientific achievements, cornerstones in crystallography and in neutron scattering.

The prize is awarded to a young European scientist, with a career extending to 5 to 8 years after thesis defence, in recognition of notable experimental, theoretical or methodological contributions in the field of analysis of matter using crystallographic or neutron scattering methods.

The amount of the prize is 2000 euros and the launch of the prize is sponsored by NMI3, the Neutron and Muon Integrated Infrastructure Initiative (http://neutron.neutron-eu.net). In the long term ECA and ENSA aim to make equal contributions to the financing of the prize through donations, sponsors etc.. To maintain the prize ECA and ENSA will establish a dedicated fund.

The first call for nominations is open until February 28th 2007. Details for the procedure and guidelines for application are available on the web-sites of ECA (http://www.ecanews.org/) and ENSA (http://neutron.neutron-eu.net/n_ensa/). The first prize will be distributed at the European conference for Neutron Scattering in Lund, Sweden, June 25-29, 2007 (http://www.ecns2007.org).

// 5th PSI Summer School on Condensed Matter Research, Zuoz, Switzerland //

S. Janssen, K. Clausen
NUM Department, Paul Scherrer Institut, CH-5232 Villigen PSI

Once a year the Paul Scherrer Institut organizes its tradional summer schools on condensed matter research at the 'Lyceum Alpinum' in Zuoz, Engadin valley. While the experimental methods provided by PSI to the scientific community, that is neutrons, muons and synchrotron light play a crucial but not exclusive role, the emphasis of the school is on a particular topic, to be defined every year. The topic of the fifth school (2006) was 'Neutron, X-ray and Muon Studies of Nano Scale Structures' with a special emphasis on 'Soft Condensed Matter Systems'. As usual the school was mainly addressed to the education of PhD and postdoctoral students without prior knowledge of neutron, X-ray and muon techniques.

The program started with introductory courses on X-ray and neutron sources by L. Rivkin and K. Clausen, respectively, followed by two lectures on 'Elementary Scattering' given by J. Mesot (neutron part) and J.F. van der Veen (X-ray part).

The second part of the school was then devoted to the various neutron, X-ray and muon techniques, which are relevant for the field. T. Prokscha and R. Scheuermann shared the introduction to 'muon spin rotation' and presented various relevant scientific examples. T. Gutberlet and P. Müller-Buschbaum (TU München) gave presentations on 'Reflectometry' and 'Grazing Incidence Small Angle Scattering', respectively, before J. Kohlbrecher talked about the general aspects of 'Small Angle Scattering'. All those introductory lectures on the techniques were accomplished by practical sessions, where the students could either deepen the content of the lectures or where they received important additional information about the practical aspects of related experiments and data analysis.

The remaining part of the school contained scientific presentations on 'hot topics' from the field of 'Nano Scale Structures and Soft Condensed Matter':

- Protein Crystallography (E. Pohl, PSI Villigen)

The participants of the 5th summer school in Zuoz in front of the Lyceum Alpinum.

- Small Angle Scattering from Biological Macromolecules
  (D. Svergun, EMBL/DESY, Hamburg)
- Proteins: From Model Colloids to Cataract Formation
  (A. Stradner, University of Fribourg)
- Bio-Membranes
  (H. Wacklin, University of Oxford)
- Membranes (K. Mortensen,
  Danish Polymer Centre, Risø)
- X-ray and Neutron Scattering Studies of Polymers
  (I.W. Hamley, University of Reading)
- Polymer Dynamics Studied by Inelastic Neutron Scattering
  (R. Zorn, Forschungszentrum Jülich)
- Dynamics of Macromolecular Systems Studied by μSR
  (I. McKenzie, University of Stuttgart)
- Fibre Diffraction Using X-rays and Neutrons (T. Forsyth, ILL Grenoble)
- Colloids
  (S. Egelhaaf, University of Düsseldorf)
- Theory of Colloids
  (M. Fuchs, University of Konstanz)

The evening sessions in Zuoz traditionally contain presentations on very interesting topics and tend to have the character to be highlights of the schools. Also in 2006 those presentations were very stimulating: Two evenings were dedicated to the fascinating and evolving field of imaging techniques. E. Lehmann talked about 'Options, Performance and Limitations of Neutron Imaging Systems' and M. Stampanoni presented a 'Fascinating Trip from Macro to Nano by X-ray Imaging'. The third evening presentation was given by F. Pfeiffer on the possibilities offered by the technique of 'Coherent X-ray Scattering'.

The school ended with a Biologist's point of view on the physical techniques presented during the school: K. Ballmer gave a presentation entitled 'New Tricks to Solve Biological Problems: What Biologists Expect from Physics'.

Done! The hiking tour group on the summit of 'Piz Languard'.

The students did not only listen to the presentations but could also present their scientific activities in a dedicated poster session with 35 posters in total. That session gave also the opportunity to discuss with the speakers and to create new contacts.

The school was attended by totally 87 participants, which is well in agreement with the average participant numbers of the previous years. Those 87 participants consisted of 11 master students, 34 Ph.D. students, 10 Post Docs, 29 senior scientists including the invited lecturers and 3 participants with a status different from the categories mentioned before. Naturally most of the participants were affiliated to Swiss institutions (44%) followed by Germany (22%), Italy (7%), United Kingdom (6%) and Russia (5%). In total participants from 15 different countries attended the school.

The complete program of the school is online available together with pdf-versions of all given presentations from: http://num.web.psi.ch/zuoz2006/

From the very beginning of the PSI summer schools it was always aimed by the organizers to stimulate not only the scientific exchange but also to offer an interesting social program with mainly sporting activities in the fascinating environment of the Alpes around Zuoz. The tradition of the free afternoons was kept also in 2006 and the participants could choose between various activities such as excursions to the nearby 'National Park', a mountain hiking tour to the 'Piz Languard' guided by H. Grimmer or to play tennis on the traditional courts of the Lyceum. Those who were particularly courageous could even show their ability in the discipline of 'River Rafting'.

We thank the school secretary Mrs Renate Bercher for the perfect organization and support before, during and after the school. Furthermore financial support by the European Commission under the 6th Framework Programme through the Key Action: Strengthening the European Research Area, Research Infrastructures, Contract n°: RII3-CT-2003-505925' (NMI3) is gratefully acknowledged.

Some of the 'non-hydrophobic' participants during their 'River Rafting' adventure.

// Conferences and Workshops 2007 //

(an updated list with online links can be found here: http://sinq.web.psi.ch/sinq/links.html)

JANUARY

International Workshop on Current Challenges in Liquid and Glass Science
January 10-12, 2007, The Coseners House, Abingdon, England

International Workshop on Advanced Laue Diffraction in Frontier Science
January 23-27, 2007, Grenoble, France

First European XFEL Users Meeting
January 24-25, 2007, Hamburg, Germany

DMM 2007: Dynamics of Molecules and Materials
January 31 - February 2, 2007, Grenoble, France

FEBRUARY

Annual Meeting of the Swiss Physical Society
February 20-21, 2007, University of Zurich, Switzerland

28th HMI School on Neutron Scattering
February 26 - March 2, 2007, HMI Berlin, Germany

MARCH

NOP 07: European Workshop on Neutron Optics
March 5-7, 2007, PSI Villigen, Switzerland

MAY

GISAXS – an advanced scattering method
May 9-11, 2007, Hamburg, Germany

SCES 07 – International Conference on Strongly Correlated Electron Systems
May 13-18, 2007, Houston, USA

BENSC Users Meeting 2007
May 23-25, 2007, HMI Berlin, Germany

ICCS 2007: International Conference on Computational Science
May 27-30, 2007, Beijing, China

JUNE

Engineering of Crystalline Materials Properties: State-of-the-Art in Modeling, Design, and Applications
June 7-17, 2007, Erice, Italy

1st School and Workshop on X-ray Micro and Nanoprobes: Instruments, Methodologies and Applications
June 11-17, 2007, Erice, Italy

ECNS 2007: 4th European Conference on Neutron Scattering
June 25-29, 2007, Lund, Sweden

9th SINQ Users' Meeting, Satellite Meeting of ECNS 2007
Between June 25-29, 2007, Lund, Sweden

ICNM-2007: 4th International Conference on Nanoscaled Magnetism
June 25-29, 2007, Istanbul, Turkey

JULY

NIB 2007: Neutrons in Biology
July 11-13, 2007, Rutherford Appleton Laboratory, Oxfordshire, UK

AUGUST

6th PSI Summer School on Condensed Matter Research
August 18-25, 2007, Zuoz, Switzerland

ECM24: 24th European Crystallographic Meeting
August 22-27, 2007, Marrakech, Morocco

Diffusion Fundamentals II
August 26-29, 2007, L'Aquila, Italy

SEPTEMBER

Annual Meeting of the Swiss Society for Crystallography
September 10-11, 2007, PSI Villigen, Switzerland

8th SLS Users' Meeting
September 11-12, 2007, PSI Villigen, Switzerland

DyProSo XXXI: 31st International Symposium on Dynamic Properties of Solids
September 25-29, 2007, Porto, Portugal

Swiss Neutron Scattering Society
Sekretariat SGN/SSDN
Paul Scherrer Institut
bldg. WLGA/002
5232 Villigen PSI, Switzerland